Title
Greenness, texture, and spatial relationships predict floristic diversity across wetlands of the conterminous United States

Authors
Taddeo, Sophie
Dronova, Iryna
Harris, Kendall

Publication Date
2021-05-01

DOI
10.1016/j.isprsjprs.2021.03.012

Peer reviewed

Title: Greenness, Texture, and Spatial Relationships Predict Floristic Diversity Across Wetlands of the Conterminous United States

Sophie Taddeo[1,2*], Iryna Dronova[3,4], and Kendall Harris[4]

[1] Negaunee Institute for Plant Conservation Science and Action, Chicago Botanic Garden, 1000 Lake Cook Road, Glencoe, IL, 60022 U.S.A. ORCID: 0000-0002-7789-1417

[2]Plant Biology and Conservation, Weinberg College of Arts & Science, Northwestern University

[3]Department of Environmental Science, Policy and Management, Rausser College of Natural Resources, University of California Berkeley, Berkeley, California 94720-3114 USA. ORCID: 0000-0003-3339-3704

[4]Department of Landscape Architecture & Environmental Planning, College of Environmental Design, University of California Berkeley, Berkeley, California 94720-2000 USA. ORCID: 0000-0001-7587-4237

*corresponding author: staddeo@chicagobotanic.org

Abstract

Plant diversity safeguards wetland ecosystem functions, stability, and resilience, but is threatened by habitat loss and degradation. Remote sensing could support the cost-effective management of biodiversity by providing consistent and frequent data at large scales. While identifying individual species from remote sensing with low spatial and spectral resolution data is challenging, studies can focus on factors known to correlate with or promote diversity. We tested the predictive potential of such factors — maximum annual greenness as an indicator of productivity, texture (i.e., spatial arrangements of grey tones) as a proxy for habitat heterogeneity, and spatial autocorrelation — across a dataset of 1,115 wetlands in the conterminous United States surveyed by the EPA's National Wetland Condition Assessment. We used multivariate linear regressions to test whether spectral and spatial metrics derived from two open-source datasets — NASA's Landsat 5 TM and 7 ETM+ (30m, 16-day revisit) and USDA's National Agriculture Inventory Program (1m, biennial) — can predict wetland plant diversity and richness. Individual texture metrics showed different sensitivity to vegetation evenness, growth form, and spatial distribution and could together predict 35-36% of site variation in richness and diversity. This highlights the impact of habitat heterogeneity on species diversity and spectral variability. While maximum annual greenness and texture metrics had similar predictive capacity, their interactions and combined effects improved the fit of linear models by 11-14%, demonstrating their complementarity.

Best results were achieved when including distance-based Moran Eigenvector Maps (dbMEMs) describing spatial relations among sites at multiple scales and reflecting the role of spatially structured factors (e.g., climate, topography, dispersal) on diversity. Together greenness, texture, and dbMEMs could predict 59% of plant richness and 50% of plant diversity across the entire dataset and up to 71% of the richness of least disturbed sites. These results show the potential of open-source remote sensing datasets to monitor biodiversity resources at a large scale and prioritize the protection and field monitoring of wetlands.

Keywords: remote sensing, distance-based Moran Eigenvectors Maps, National Agriculture Inventory Program, Landsat, National Wetland Condition Assessment, spectral heterogeneity

Abbreviations

Distanced-based Moran's eigenvector maps (dbMEMs)
Green Normalized Difference Vegetation Index (GNDVI)
National Agriculture Inventory Program (NAIP)
National Wetland Condition Assessment (NWCA)
Near infrared (NIR)
Spectral Vegetation Indices (SVI)

1 Introduction

1.1 Importance of biodiversity

Theoretical and experimental studies have demonstrated the crucial role of biodiversity in promoting ecosystem productivity, stability, and resilience (Cardinale et al., 2012; Hooper et al., 2012, 2005). Wetlands support a diversity of organisms at several trophic levels (Kingsford et al., 2016), sheltering over one third of species listed as threatened or endangered in the United States (Niering, 1988). Yet wetlands are declining at a greater rate than most terrestrial habitats, making them one of the most stressed ecosystems in the world (Davidson, 2014; Dudgeon et al., 2006; Gibbs, 2011). Their rate of degradation is likely to accelerate with climate change exacerbating droughts, floods, and sea level rise (Craft et al., 2009; Shepard et al., 2011) while increasing human needs for the ecosystem services they provide (e.g., flood control, carbon sequestration, water filtration; Chmura et al., 2003; Costanza et al., 2008; Zedler, 2003). Protecting wetlands and restoring degraded sites is thus crucial to ensure the long-term persistence of their biological diversity and the ecosystem services it provides (Dudgeon et al., 2006).

1.2 Large scale monitoring of wetland diversity

As wetland conservation resources are scarce (Kingsford et al., 2016), it is pivotal to develop methodologies enabling the rapid assessment of biodiversity at high frequency, large scales, and low cost (Pereira et al., 2013). Yet current monitoring efforts tend to be limited in coverage and difficult to upscale due to varying methodologies and taxonomic focus (Pereira and Daily, 2006). As a result, it becomes difficult to identify priority areas where conservation interventions are most needed or likely to be rewarding. Remote sensing products, some of which offer a global coverage at frequent time intervals (e.g., Landsat, MODIS, Sentinel-2), can help monitor diversity by providing consistent low-cost primary data thus bridging gaps between smaller-scale in situ biodiversity assessments (Pereira and Daily, 2006).

However, identifying individual species or measuring their diversity from satellite images is challenging, particularly when using multispectral broadband data (i.e., spectral signal summarized within fewer bands integrating wider portions of the electromagnetic spectrum), a medium to coarse resolution (>30m), or when focusing on heterogeneous environments such as wetlands (Andrew and Ustin, 2008; Bradley, 2014; Turner et al., 2003). Differentiating individual species is most effective when using high resolution (<1m) or hyperspectral data (i.e., spectral signal summarized within narrower portions of the electromagnetic spectrum) which can best detect chemical differences among species (Andrew et al., 2014; Ustin and Gamon, 2010). At coarser resolutions (e.g., Landsat's 30m), the background effect of non-vegetated surfaces including open water and bare soil can obscure plant reflectance (Andrew and Ustin, 2008; Schmidt and Skidmore, 2003). To overcome these limitations, recent efforts have sought to estimate biodiversity from its known associations with ecosystem properties (e.g., Castillo-Riffart et al. 2017; Madonsela et al. 2017; Taddeo, Dronova, and Harris 2019) or by using broadband, multispectral, and medium-high resolution data to measure ecosystem/landscape factors known to promote diversity (Turner et al., 2003).

1.2.1 Diversity-productivity relationships

A prime example of such applications is the use of spectral vegetation indices (SVI) as a proxy for species diversity. This application is rooted in the diversity-productivity theory, which posits that sites with a higher plant richness should maintain a greater productivity due to a more efficient partitioning and use of resources in time and space (Hooper et al., 2005; Tilman et al., 1996). From a remote sensing perspective, this means that high values for a SVI sensitive to plant coverage, biomass, or photosynthetic activity (Huete et al., 1997) should correlate to species richness. This theory has been tested in a variety of ecosystems (Castillo-Riffart et al., 2017; Madonsela et al., 2017) including wetlands (Taddeo et al., 2019b) with sometimes modest yet significant results demonstrating the utility of this approach to help target field monitoring and conservation interventions.

1.2.2 Texture and habitat heterogeneity

Alternative approaches involve using remote sensing indices as proxy for site and landscape factors known to promote plant diversity. Habitat heterogeneity (i.e., variety of habitat types and characteristics) stimulates biodiversity by providing distinct ecological niches enabling more species to co-exist (Deutschewitz et al., 2003; Gould, 2000). The spectral variability hypothesis postulates that species richness and habitat heterogeneity should linearly increase spatial variability in spectral signal due to species- and habitat-specific differences in chemical composition, productivity, phenology, and exposure to background land covers (Palmer et al., 2002). Some researchers have used texture metrics describing variations in the grey tones of aerial images (Hall-Beyer, 2007; Haralick, 1979) as an indicator of within-patch habitat heterogeneity to indirectly predict diversity (Hernández-Stefanoni et al., 2012; Wood et al., 2013).

In wetlands, including spectral heterogeneity in biodiversity estimates might differentiate sites with low plant diversity, greenness, and coverage (Fig. 1A) from sites with high diversity but a patchy vegetation distribution (Fig. 1C). In the latter case, the background effects of soil, water, and litter might obscure high but localized productivity and diversity, thus reducing SVI values and their effectiveness as a proxy of diversity-productivity relationships (Fig. 1). As such, using a model that combines texture (as a proxy of spectral heterogeneity) and greenness (related to biodiversity effects on plant biomass and coverage) might account for both the effect of the diversity-productivity relationship and habitat heterogeneity. Incorporating texture as a proxy for habitat heterogeneity may also help address an important challenge in the application of the diversity-productivity theory in monodominant wetlands covered by few invasive species associated with high greenness values (e.g., EVI; NDVI) but low species richness (Fig. 1B; Taddeo et al., 2019b). Highly invaded sites, however, might have a low spectral heterogeneity which could be captured by textural metrics.

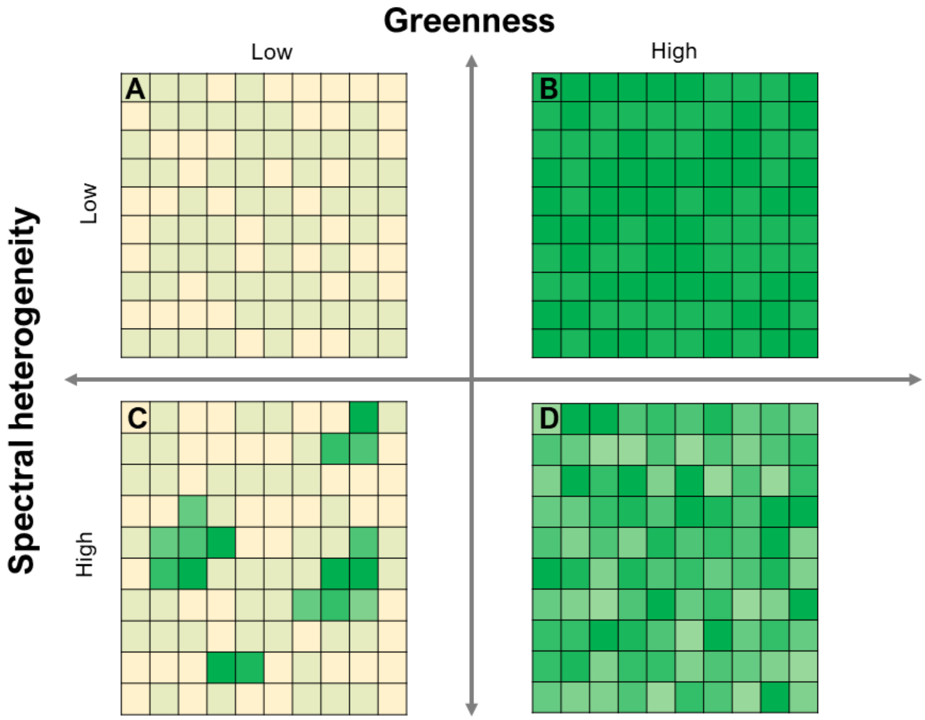

Figure 1: Conceptual model describing the potential relationship between site greenness, spectral heterogeneity, and species richness. (A) Disturbed site with a low overall greenness, spectral heterogeneity, and species diversity. (B) Site with monodominant non-native species resulting in high greenness and low spectral heterogeneity. (C) Local stressors (e.g., salinity, flooding) result in low overall greenness but high spectral heterogeneity and high, but localized, species diversity. (D) Resource-abundant site with high greenness, spectral heterogeneity, and species diversity.

1.2.3 Spatial autocorrelation

Spatial autocorrelation, or the degree of similarity among plant communities in close proximity, could also improve biodiversity estimates (e.g., Kreft and Jetz 2007). Spatially structured local (e.g., soil, topography) and regional abiotic characteristics (e.g., climate) influence species composition and diversity resulting in their positive spatial autocorrelation (i.e., similarity). Meanwhile, physical barriers limiting species dispersal (Karst et al., 2005) and disturbances impacting plant persistence (Biswas et al., 2016) can result in a negative spatial autocorrelation (i.e., distinctiveness in site composition and diversity) at the local or regional scale. Recognizing that the effects of spatial autocorrelation can be both positive and negative and vary across scales, recent efforts have developed eigenfunctions describing spatial relationships (i.e., distance and connectivity) among sites (Dray et al., 2006; Peres-Neto and Legendre, 2010). These multi-scale predictors can be incorporated in models predicting diversity to account for the influence of spatially-structured variables and disturbances on plant assembly (e.g., Hernández-Stefanoni et al., 2012; Peres-Neto and Legendre, 2010).

1.2.4 Research goals and hypotheses

Our goal was to compare predictors (i.e., maximum annual greenness, texture, and spatial autocorrelation) of wetland plant richness and diversity derived from open-source databases. This study builds on a previous effort utilizing maximum annual greenness (i.e., maximum annual value for a spectral vegetation index sensitive to plant coverage and abundance) derived from the Landsat archive to predict plant diversity across 1,115 wetlands of the conterminous United States (Taddeo et al., 2019b). We hypothesized that a multivariate predictive model leveraging both texture and greenness (i.e., maximum SVI value) would enhance predictive potential by accounting for the positive impact of habitat heterogeneity on plant richness and minimizing the confounding effect of background land covers (e.g., soil, water, litter) and introduced species on diversity-productivity relationships. Our previous effort did incorporate standard deviation in maximum greenness measured from Landsat data as a predictor of species richness, with a significant but somewhat low predictive capacity (i.e., standard deviation in maximum greenness estimated using the Green Normalized Vegetation Index could predict 3% of variation in site richness; Taddeo et al., 2019b). In the present study, we explored this potential more in-depth by testing a greater range of texture measures representing complementary aspects of spatial heterogeneity. Finally, we expected that including spatial autocorrelation in models would enhance their predictive capacity by accounting for the positive impact of spatially structured abiotic conditions (temperature, precipitations) on wetland plant diversity.

2 Methods

2.1 Study area and sites

Our study leverages species composition and coverage data collected by the U.S Environmental Protection Agency's National Wetland Condition Assessment (NWCA) during peak growing season in the spring and summer of 2011 in 1,138 wetlands of the conterminous United States (Fig. 2). We excluded 23 sites that were not covered in 2010 nor 2011 by the National Agriculture Inventory Program (NAIP), the dataset of higher resolution (1m) aerial images used in this study to compute texture metrics. Wetlands sampled by the NWCA are stratified by state (≥ 8 sites per state) and wetland type to represent the broader population of wetlands in the United States (US EPA, 2016).

Wetlands are classified into four general types based on their hydrological characteristics and dominant vegetation (Fig. 2; US EPA 2016): estuarine herbaceous (EH; n=270) and inland herbaceous (PRLH; n=350) wetlands dominated by emergent herbaceous species, estuarine woody wetlands dominated by small trees and shrubs (EW; n=70), and inland woody wetlands including both forested and scrub-shrub wetlands (PRLW; n=425). NWCA sites are also grouped in three categories along a disturbance gradient — least disturbed (n=273), intermediate (n=518), and most disturbed (n=324) — based on anthropogenic structures (e.g., agriculture, timber, urban development), hydrological disturbances (e.g., ditches, dams, levees), heavy metal concentration, and introduced species (US EPA, 2016).

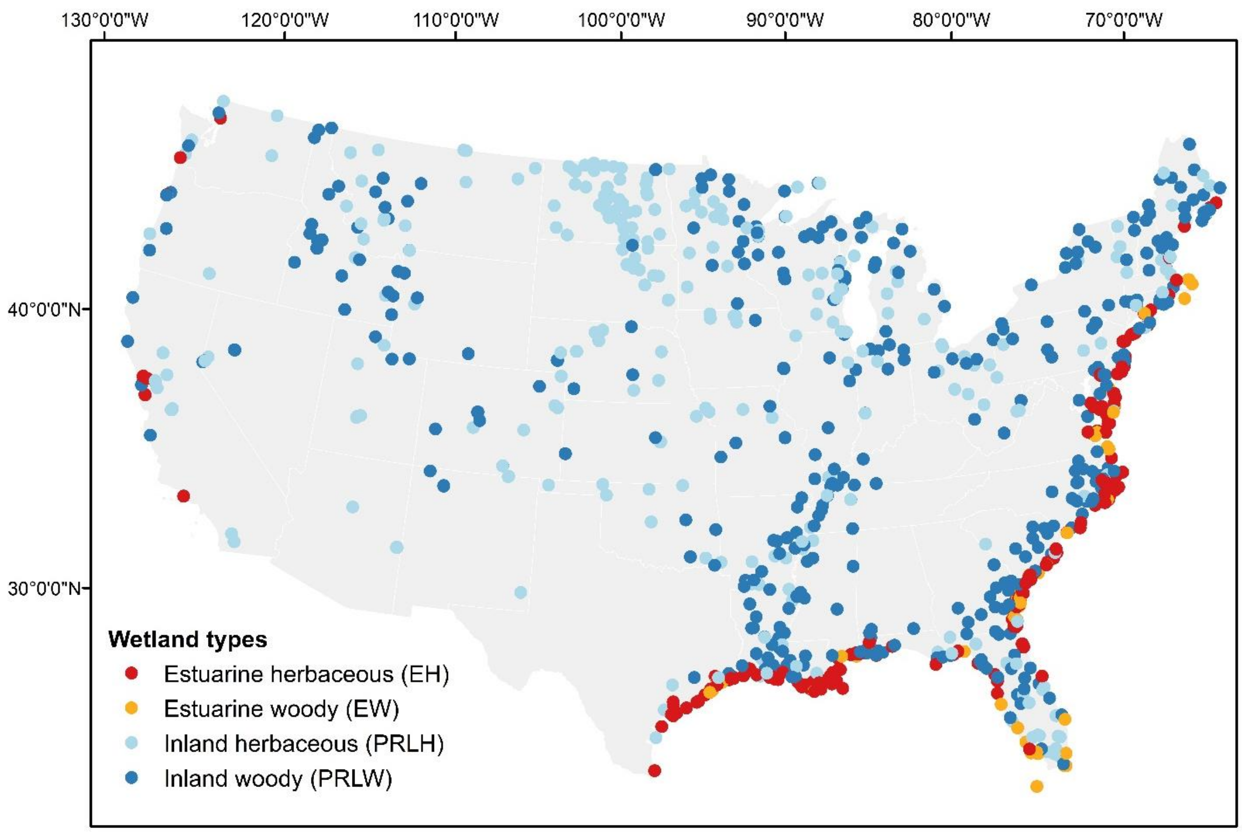

Figure 2. Wetland sites surveyed in 2011 by the US EPA's National Wetland Condition Assessment (NWCA), by wetland type (i.e., aggregated wetland classes as defined in the NWCA).

2.2 In situ biodiversity and abiotic data

The NWCA surveyed species cover and composition in five 100m^2 plots per site included in a 0.5 ha assessment area (US EPA, 2016). Two sites per state (n=96) were visited a second time in the same year to assess the stability of previous observations and showed a high correlation between floristic characteristics measured during the first and second visit (US EPA 2016; SI Table S1). In this study, we focused on three diversity indicators derived from the NWCA first visits: the Shannon-Wiener Diversity Index, total species richness, and the richness of native species (Table 1). These metrics were calculated from the entire list of vascular plant species observed across the five sampling plots of a site's assessment area (US EPA, 2016). The NWCA labeled species as "native" when they were native to the state in which they were found based on the U.S Department of Agriculture PLANTS database and state-specific floristic databases (US EPA, 2016). The term “alien species” refers to both introduced species (i.e., plant species introduced from outside the conterminous United States) and adventive species (i.e., plant species native to some portions of the United States but introduced to the state in which their presence was recorded).

Table 1. In situ variables (i.e., vegetation characteristics extracted from the NWCA) used for this analysis with the acronyms used to identify them in the NWCA.

Category	Variable	Description
Species diversity	Shannon-Wiener Diversity Index (H_ALL)	Diversity of species
	Total Species Richness (TOTN_SPP)	Count of unique species
	Native Species Richness (TOTN_SPP)	Count of unique native species
	Percent Alien Species Richness (PCNT_ALIEN)	Percent of total richness associated to alien species
Vegetation coverage	Total vegetation coverage (XTOTABCOV)	Total vegetation coverage
	Coverage of native species (XABCOV_NATSPP)	Total vegetation coverage of native species
	Coverage of non-native species (XABCOV_ALIENSPP)	Total vegetation coverage of non-native species

2.3 Spectral and Texture Indicators

2.3.1 Site Greenness

We used the Green Normalized Difference Vegetation Index (GNDVI) —based on the normalized difference between the green band, sensitive to species-specific variation in chlorophyll content, and the near infrared (NIR) band, strongly reflected by mesophyll cells — as an indicator of plant biomass and coverage (Gitelson and Merzlyak, 1998; here after referred to as "greenness"). GNDVI was the best predictor of plant richness and diversity in this dataset among a group of six SVIs (Taddeo et al., 2019b). Remote sensing images were processed in the cloud based platform Google Earth Engine (Gorelick et al., 2017). We estimated GNDVI at the pixel level for all Landsat 5 TM and 7 ETM+ cloud-free images captured in 2011 and overlapping the NWCA sites (Taddeo et al., 2019b). We leveraged the quality assessment band of the Landsat 5 TM and 7 ETM+ surface reflectance products to mask pixels with clouds or cloud shadows in the time series. We computed GNDVI for nine Landsat pixels (30m) overlapping each site, which roughly corresponds to the 0.5-acre assessment used by the NWCA (Taddeo et al., 2019b). We focused on the maximum GNDVI value per site (i.e., spatial average of the maximum GNDVI value observed in individual pixels) as an estimate of site productivity as it significantly predicted plant diversity in our previous study while being less sensitive to the background effect of water, soil, and litter exposure than the median value (Taddeo et al., 2019b, 2019a).

2.3.2 Texture

We used high resolution aerial images (1m) from the U.S. Department of Agriculture's National Agriculture Imagery Program (NAIP) to calculate texture metrics describing spatial heterogeneity in the reflectance of all 1m pixels included in the 0.5 ha assessment area of individual NWCA sites (~5,026 pixels per site). Texture metrics were generated in Google Earth Engine using the *glcmTexture* function. These metrics (Table 2) describe how often different combinations of grey values (i.e., digital numbers in a given band) occur together in the image (in this case, the extent of the "image" corresponds to the assessment area of a site). These metrics are second order-based, meaning that they account for the relationships (e.g., contrast, homogeneity, correlation) between a pixel and its neighbors. Texture metrics were computed for individual bands (red, blue, green, NIR) of the NAIP dataset. To reduce redundancy among these metrics, we focused on five texture metrics per band representing broad categories of metrics described by Hall-Beyer (2007): contrast, orderliness, and descriptive texture measures (Table 2). Entropy (i.e., degree of uniformity in grey tones; Guo et al. 2004) was used in this study as a metric of orderliness, dissimilarity (i.e., contrasts between neighboring pixels; Guo et al. 2004; Hall-Beyer 2017) as a measure of contrast, while correlation (linear correlation in grey tones), average (average digital number value within the assessment area), and variance (variance in digital numbers within the assessment area) were used as descriptive measures. Using the *cor.test* function in R, we measured the Pearson's correlation coefficient among all pairs of texture metrics and removed three variables with a correlation coefficient exceeding 0.8 ($p<0.05$): sum average in the NIR band, sum average in the green band, and entropy in the red band. Lastly, we used the *decostand* function of the *vegan* package in R (Oksanen et al., 2019) to normalize texture variables prior to conducting linear regressions.

Table 2. Texture metrics computed for this analysis and their interpretation

Category	Texture metric	Description	Interpretation
Contrast	Dissimilarity	Measures contrast in the grey-tone of neighboring pixels	High value indicates an important local contrast between neighbors
Orderliness	Entropy	Measures the degree of randomness in the distribution of pairs of grey tones	Low entropy value suggest uniformity in clusters of grey tones (i.e., clusters of grey tones are repeated throughout the image)
Descriptive	Sum average	Mean grey tone value across an image	Magnitude of reflectance in each band at the image scale
	Sum Variance	Variance in grey tones within an image	Greater variance suggests a greater dispersion of grey tone values within the image
	Correlation	Linear correlation between the grey-tone values of an image	Predictability in the grey-tones of neighboring pixels

2.4 Spatial analyses

We used distanced-based Moran's eigenvector maps (dbMEMs) to assess the impact of spatial autocorrelation (i.e., how similarity in plant richness and diversity varies with distance among sites) on plant diversity. The dbMEM approach produces a set of uncorrelated spatial predictors that can be integrated in explanatory models to account for the effect of spatial phenomenon (e.g., dispersal, competition at a local scale, climate at a broader scale) on species composition and diversity (Peres-Neto and Legendre, 2010). To generate dbMEMs, users must first produce a truncated matrix of Euclidean distances among all pairs of sites (Dray et al., 2006; Peres-Neto and Legendre, 2010). Spatial eigenvectors are then generated from the resulting matrix with the first few eigenvectors representing broad spatial relationships (i.e., distance among sites at different scales) while the last eigenvectors describe local spatial relationships (SI Fig. S4). dbMEMs were calculated in R 3.6.2 using the *dbmem* function of the *adespatial* package (Dray et al., 2018). Lastly, for each individual predictive model (i.e., species diversity and richness) we used the *forward.sel* function of the *adesaptial* R package (Dray et al., 2018) to select the most parsimonious model (i.e., minimum number of dbMEMs for the highest explanatory power). *Forward.sel* iteratively adds explanatory variables to a predictive model until the adjusted R^2 of the global model (i.e., model with all explanatory variables) is reached (Dray et al., 2018). After determining the most parsimonious combination of dbMEMs to predict the richness and diversity of the entire dataset, specific wetlands types, and disturbance levels, we visually grouped the dbMEMs into four scales — broad, medium, fine, very fine — to test which scale of spatial relationships had the strongest incidence on floristic diversity (SI Fig. S4).

2.5 Statistical analyses

We used univariate (e.g., maximum annual greenness, individual texture metrics) and multivariate (e.g., texture metrics, dbMEMs) linear regressions to identify the best predictors of the Shannon-Wiener diversity index, total species richness, and the richness of native species. Species richness and native species richness were both log-transformed as they had a skewed distribution. Three groups of variables were used as predictors in multivariate linear regressions. The "greenness" group refers to the maximum GNDVI detected in 2011 and averaged over the nine Landsat pixels overlapping each NWCA site. The "texture" group includes 17 uncorrelated texture metrics (Table 2) derived from the NAIP dataset. The dbMEM group includes dbMEMs generated for the entire dataset with a forward selection to only include a most parsimonious subset of variables. Linear regressions were conducted in R using the *lm* function. We report in this paper the adjusted R^2 of relationships and their p-value (significant when $p<0.05$). We used the *dcor* function of the *energy* R package (Rizzo and Székely, 2018) to examine non-linear relationships between maximum annual greenness and individual texture metrics by measuring their distance correlation, which is computed by comparing the distance between the X values of a pair of observations and their Y values (Székely et al., 2007). A distance correlation (dcor) of 1 indicates a strong nonlinear relationship among two variables. Finally, we used the non-parametric Kruskal-Wallis test with Bonferroni multi-comparison correction to assess the significance of greenness and textural differences among the four wetland types. We focused on six texture metrics with the strongest predictive power in univariate predictive models (SI Table S2). This step was used to assess the sensitivity of individual texture metrics to patterns of vegetation distribution and growth forms specific to each wetland type. Analyses were conducted using the *dunn.test* R package.

3 Results

3.1 Relationships between greenness and texture

Individual texture metrics showed a non-significant to low significant (SI Table S3) linear correlation with maximum annual greenness and, generally, a low non-linear correlation (SI Fig. S1) as measured by their distance correlation. Among all texture metrics, entropy — and particularly entropy in the blue (dcor = 0.30), green (dcor =0.48), and NIR bands (dcor = 0.36) — showed the highest non-linear correlation with greenness, with higher entropy generally corresponding to a higher greenness. Dissimilarity also tended to increase with maximum greenness (with distance correlation coefficients varying between 0.29 and 0.34; SI Fig. S1). Similarly, sum variance (indicating the amount of spatially variability in grey tones) was generally associated with higher maximum annual greenness (distance correlation varying between 0.29 and 0.39). Lastly, the sum average in different bands and the correlation in band value all showed the lowest non-linear correlations with maximum annual greenness.

3.2 Textural differences between wetland types

Kruskal-Wallis tests with Bonferroni multiple test correction revealed significant contrast in the greenness (χ^2=455.13, df=3, p<0.0001; Fig. S2A) and texture of the different wetland types (Fig. 3) included in this study. Inland wetlands dominated by woody vegetation were characterized by a significantly greater greenness (p<0.0001), followed by inland herbaceous wetlands, estuarine woody, and estuarine herbaceous wetlands (SI Fig. S2A). Wetland types also differed in their entropy in the green band (χ^2=373.93, df=3, p<0.0001; Fig. 3A), dissimilarity in the NIR band (χ^2=259.28, df=3, p<0.0001; Fig. 3B), variance in the green band (χ^2=306.66, df=3, p<0.0001; Fig. 3C), dissimilarity in the red band (χ^2=220.63, df=3, p<0.0001; Fig. 3D), variance in the NIR band (χ^2=211.15, df=3, p<0.0001; Fig. 3E), and the variance in the red band (χ^2=195.76, df=3, p<0.0001; Fig. 3F). Inland and estuarine wetlands dominated by woody vegetation both showed significantly greater entropy in the green band (p<0.0001;

Fig. 3A) than herbaceous-dominated wetlands, indicating a greater heterogeneity in assemblages of green values, while herbaceous wetlands were characterized by a greater orderliness. Wetlands dominated by woody species (i.e., inland woody and estuarine woody wetlands) showed a greater dissimilarity in the NIR ($p<0.0001$; Fig. 3B) and red ($P<0.001$; Fig. 3D) bands than sites dominated by herbaceous species indicating a higher contrast between neighboring pixels. Lastly, inland woody wetlands were characterized by a greater sum variance in the green ($p<0.0001$; Fig. 3C), NIR ($p<0.0001$; Fig. 3C) and red bands ($p<0.0001$; Fig.3F), indicating higher overall local spectral variability in this wetland type.

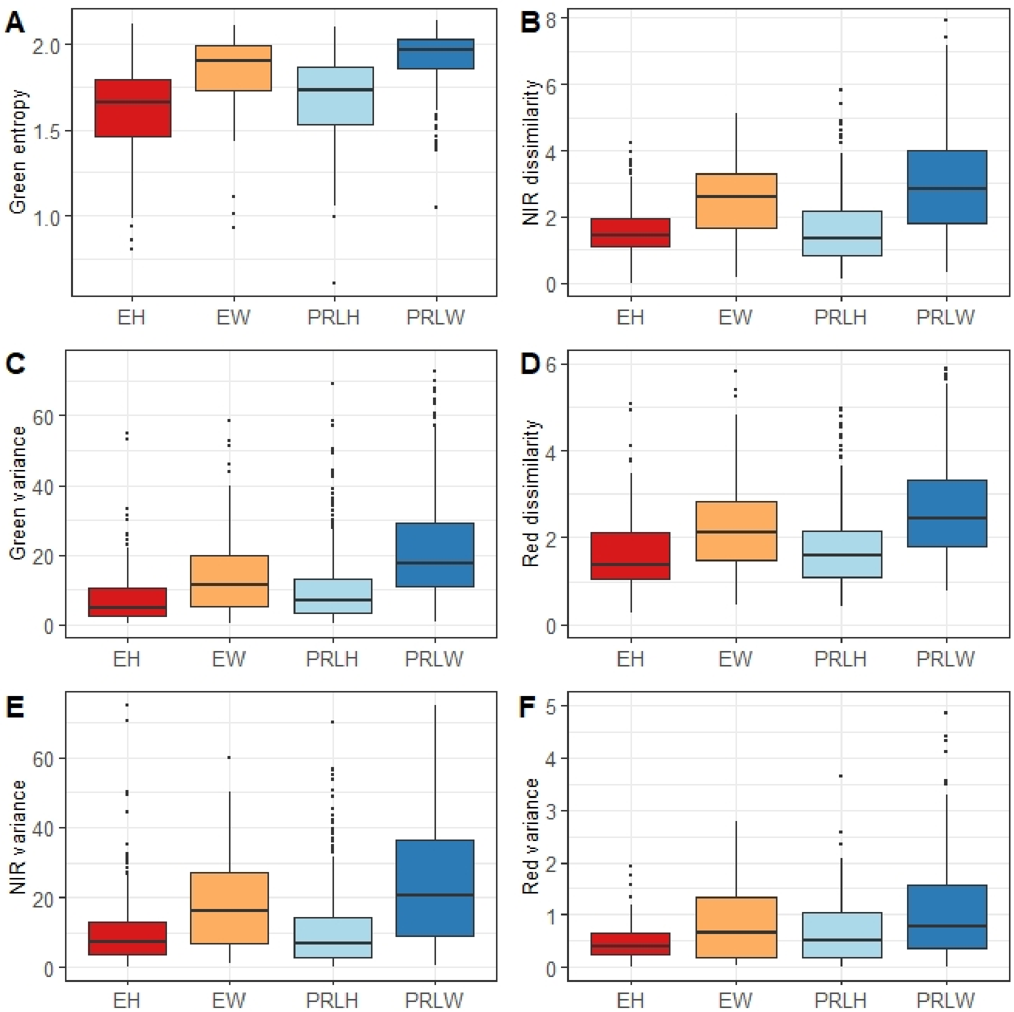

Figure 3. Textural differences by wetland type where EH are estuarine herbaceous wetlands, EW are estuarine woody wetlands, PRLH are inland herbaceous wetlands and PRLW are inland woody wetlands. Texture metrics represented in this figure are the six best individual predictors of species richness and diversity, as presented in SI Table S2.

3.3 Predictors of biodiversity

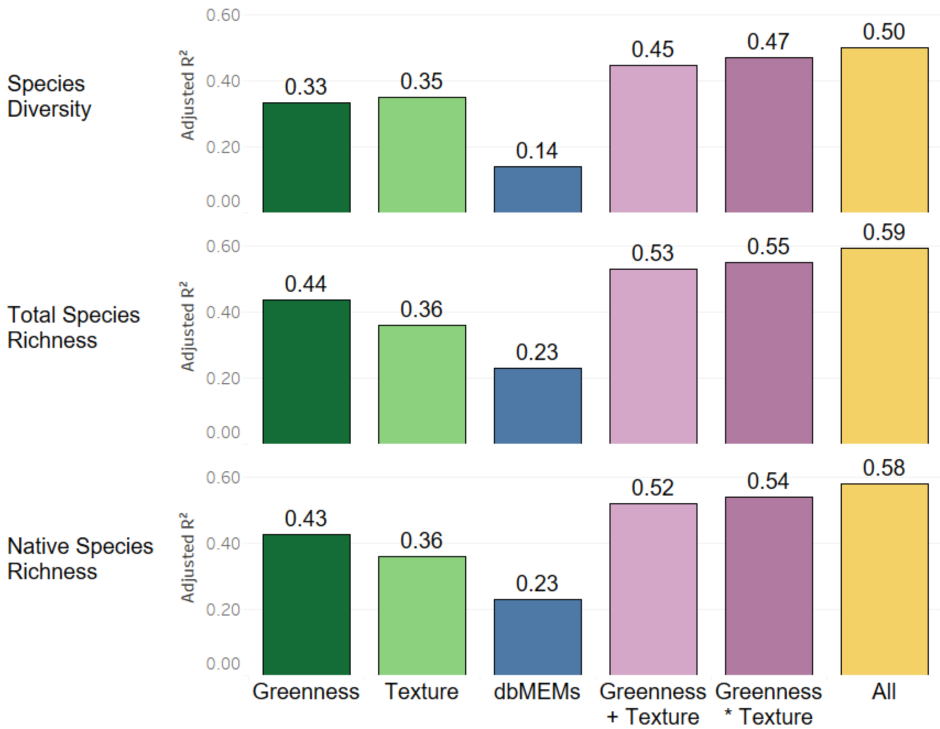

Figure 4. Proportion of variation in plant diversity and richness explained by different groups of explanatory variables as measured by their adjusted R^2.

3.3.1 Multivariate models

Texture metrics could explain 35% of variation in the species diversity of the entire dataset ($F_{17,1097}$=36.64, adjR^2=0.35, p<0.0001; Table 3; Fig. 4), which according to an ANOVA test was significantly greater than the proportion of variance explained by maximum greenness alone (ANOVA test; F_{16}=3.09, p<0.0001). Texture could improve the capacity of the greenness model to predict species diversity by 12% (ANOVA test; F_{17}=14.27, p<0.0001). However, greenness-only and texture-only models did not significantly differ in the capacity to predict species richness despite their 8% difference in adjR^2 (Table 3; Fig. 4). Incorporating texture to the greenness model significantly improved its capacity to predict the richness of all species (ANOVA test; F_{17}=13.66, p<0.0001) by 9%. Similarly, the capacity of the greenness-only and texture-only models to predict the richness of native species did not significantly differ according to an ANOVA test (p>0.05) but incorporating texture to greenness significantly increased the fit (ANOVA; F_{17}=13.78, p<0.0001; Table 3; Fig. 4) of the model by 9%. Models accounting for the interaction between greenness and texture (greenness * texture, Table 3; Fig. 4) explained more variation in species diversity (ANOVA; F_{17}=21.59, p<0.0001), total species richness (ANOVA; F_{17}=3.91,

$p<0.0001$), and the richness of native species (ANOVA; $F_{17}=3.31$, $p<0.0001$) than multivariate models based on solely greenness and texture (greenness + texture, Table 3; Fig. 4).

The greenness-only and texture-only models did not differ significantly in their capacity to predict the richness and diversity of least disturbed sites. Texture metrics could explain 42-45% of variation in the richness and diversity of least disturbed sites and improved the fit of greenness models by 7-8% (Table 3). Similarly, greenness-only and texture-only models did not differ significantly in their capacity to predict the richness and diversity of sites with an intermediate level of disturbance, but texture metrics could improve the fit of the greenness model by 7-10% (Table 3). Texture was, however, a better predictor of the richness (ANOVA; $F_{17}=13.53$, $p<0.0001$) and diversity (ANOVA; $F_{17}=14.05$; $p<0.0001$) of most disturbed sites than greenness, explaining 39-44% of their variation (Table 3). Texture metrics explained 26-32% of variation in the richness and diversity of estuarine woody wetlands, 14-17% of variation in the richness and diversity of estuarine herbaceous wetlands, 7-13% of variation in the richness and diversity of inland herbaceous wetlands, and 12-14% of variation in the richness and diversity of inland woody wetlands (Table 3).

3.3.2 <u>Spatial relationships</u>

The most parsimonious species diversity model included 14 dbMEMs and could explain 14% ($F_{22,1092}=1.90$, $adjR^2=0.14$, $p<0.0001$) of the variation among all sites (Fig. 4; Table 3). An ANOVA test showed that including dbMEMs significantly improved the greenness + texture model (ANOVA; $F_{13}=1.47$, $p<0.0001$; Fig. 4), increasing its predictive capacity to 50%. The most parsimonious species richness model included 23 dbMEMs and could explain 23% ($F_{22,1092}=16.11$, $adjR^2=0.23$, $p<0.0001$) of the variation among all sites (Table 3). dbMEMs combined to greenness and texture explained 59% of variation in species richness ($F_{40,1074}=38.75$, $adjR^2=0.59$, $p<0.0001$), thus significantly improving the fit of the model (ANOVA; $F_{22}=7.32$, $p<0.0001$; Fig. 4; Table 3). The most parsimonious native species richness model included 25 dbMEMs and could explain 23% of the variation among all sites ($F_{24,1092}=14.73$, $adjR^2=0.23$, $p<0.0001$; Fig. 4; Table 3). dbMEMs combined to greenness and texture could explain 58% of variation in native species richness ($F_{42,1072}=37.42$, $adjR^2=0.58$, $p<0.0001$), significantly increasing the fit of the linear relationships (ANOVA; $F_{24}=7.46$, $p<0.0001$). Broad scale patterns (SI Fig.S4) could explain 21.6% of variation in native species richness ($F_{44,1,108}=52.1$, $adjR^2=0.22$, $p<0.0001$). Medium-scale patterns (SI Fig.S4) could explain 4.7% of variation in species diversity ($F_{44,1,108}=10.15$, $adjR^2=0.05$, $p<0.0001$). Fine-scale patterns (SI Fig.S4) could explain 4% of variation in species diversity ($F_{44,1,177}=8.43$, $adjR^2=0.04$, $p<0.0001$). Very fine-scale (SI Fig.S4) patterns could explain 5% of variation in species diversity ($F_{44,1,100}=5.21$, $adjR^2=0.05$, $p<0.0001$).

4 Discussion

Spectral and spatial variables derived from open-source datasets could predict up to 59% of plant richness and diversity across the NWCA sample representative of the broader population of US wetlands. In least disturbed sites, this predictive capacity reached 71%. This suggests that combining texture metrics with spectral greenness and dbMEMs can predict a substantial proportion of plant diversity, even in habitats where remote sensing-based monitoring is challenged by patchy vegetation or predominance of woody species. These results highlight the potential of remote sensing in informing the field monitoring and management of wetlands and upscaling local in situ surveys of floristic diversity into regional estimates (Pereira et al., 2013; Pereira and Daily, 2006). The predictive capacity of our different sets of variables (i.e., greenness, texture, dbMEMs) varied among wetland types and disturbance levels which points to their sensitivity to different drivers of wetland heterogeneity and constraints to diversity and productivity.

4.1 Contrasts and interactions among greenness and texture

Texture metrics and maximum annual greenness did not differ significantly in their capacity to predict the species richness of the entire dataset. Yet, texture metrics were better predictors of species diversity in the entire dataset, in most disturbed sites, and in estuarine woody wetlands. While both greenness and texture metrics are sensitive to the abundance and spatial distribution of vegetation as shown by previous studies (Feilhauer et al., 2012; Taddeo et al., 2019a), their low linear and non-linear correlations (SI Table S3; Fig. S1) suggest that they ultimately vary differently across ecosystem and vegetation types, likely due to their contrasts in spatial and temporal scales and sensitivity to wetland characteristics. This suggests that texture and greenness are strongly complementary and should be considered together in efforts to monitor diversity or develop leading indicators of its change in wetlands.

Incorporating texture into greenness models increased their fit by 11-14% which shows that texture metrics might help overcome some limitations of greenness as a predictor of species richness. First, texture metrics may improve floristic diversity predictions where large monodominant colonies of alien species result in high greenness and low richness. In our previous effort (Taddeo et al., 2019b), some sites with a high coverage of alien species, high greenness, and low richness appeared as “outliers” in the relationship between greenness and richness, thus limiting its applicability as a predictor of diversity in most invaded sites. The predictive potential of texture was evident in most disturbed sites characterized by a greater coverage of alien species (Taddeo et al., 2019b; US EPA, 2016), where they explained a greater proportion of variation in diversity than greenness and improved the fit of greenness models by up to 37%. Incidentally, while both categories of inland wetlands (PRLH, PRLW; SI Fig. S2A) showed a high maximum annual greenness, inland woody wetlands showed a greater spectral heterogeneity and species richness while inland herbaceous wetlands showed a higher coverage and richness of alien species and a lower spectral heterogeneity (SI Fig. S3C;F).

Second, texture metrics derived from high resolution data may be more sensitive to vegetation coverage and diversity where vegetation extent is spatially constrained by stressors (e.g., flooding or salinity gradient). At the scale of Landsat pixels (30m), low greenness can reflect both a lower plant coverage (Fig. 1A) or a high but localized productivity (Fig. 1C) where background exposure reduces greenness (Huete et al., 1985; Taddeo et al., 2019a; Todd and Hoffer, 1998). Texture metrics computed at a higher spatial resolution might thus help distinguish scattered vegetation from high plant coverage with low overall productivity and richness, as evidenced by textural differences between the two wetland types with the lowest greenness (EW and EH; Fig. 3; SI Fig. S2A) and the strong predictive capacity of texture in estuarine woody wetlands.

Third, texture metrics were sensitive to the heterogeneity of growth forms and habitats, both of which can promote floristic diversity, as is underscored in textural differences among wetland types translating specific patterns of species distribution. While both inland wetland types were characterized by a greater greenness, inland woody wetlands showed a higher overall vegetation coverage than inland herbaceous wetlands (SI Fig. S2B), suggesting that their spectral heterogeneity is not driven by a scattered distribution of vegetation (which would result in background exposure) but by spectral differences among plant functional types. Inland woody wetlands were associated with a greater dissimilarity, which indicate high local contrasts in the NIR portions of the electromagnetic spectrum (Guo et al., 2004; Hall-Beyer, 2017). The difference in NIR reflectance between woody vegetation and co-occurring herbaceous species (Asner, 1998) might explain the prevalence of this local contrast. It is also possible that high-resolution images, even with a poorer temporal frequency, can improve the predictive capacity of multivariate models in sites dominated by woody vegetation. At the scale of Landsat data, prevalence of dense woody vegetation in mixed pixels can obscure herbaceous vegetation, but texture metrics might be more sensitive to variation in species diversity within both herbaceous and woody canopies.

Finally, texture metrics were a better predictor of the Shannon-Wiener diversity index than greenness across the entire dataset and in most disturbed wetlands. This may reflect the sensitivity of texture metrics to the effect of plant dominance on diversity which richness indicators alone would not capture. When a dominant species reduces diversity without affecting the total species count, texture metrics including dissimilarity and entropy could be impacted without affecting the overall site greenness. Our results suggest that these signatures of local plant dominance, and their impact on plant diversity, may also be easier to capture using high resolution aerial images (NAIP; 1m) rather than maximum greenness estimations based on coarser data (Landsat; 30m).

While texture metrics can overcome some limitations of greenness as a predictor of diversity, the latter might be sensitive to properties of diverse wetlands that may not otherwise be captured by the single-date images we used to generate texture metrics. Both our multivariate linear models and variance partitioning (SI Fig. S3) suggest that accounting for the interactions between greenness and texture increases the predictive capacity of diversity models. At a high greenness, incorporating texture metrics might help separate the positive impact of diversity on productivity (Fig. 1D) from high greenness attributed to few monodominant but highly productive species (Fig. 1C). Meanwhile, high spectral heterogeneity might result from both a scattered vegetation (Fig. 1C) or the assembly of species associated to different spectral properties (Fig. 1D) but different maximum greenness. In addition, the low correlation between sum average in the green and NIR bands of NAIP images and the maximum GNDVI estimated from Landsat (Fig. S1) suggests that these metrics have different sensitivities to maximum biomass, possibly resulting from variations in the timing of NAIP image acquisition which does not always correspond to peak wetland greenness (SI Fig. S5).

4.2 Predictive capacity of dbMEMs

Spatial relationships among sites (i.e., their connectivity at different scales), as modeled by distance-based Moran Eigenvector Maps, capture drivers of diversity that may not be reflected in texture nor greenness. This is evidenced in the results of the variance partitioning (SI Fig. S3) which shows that 3-5% of variation in richness and diversity is uniquely explained by dbMEMs (i.e., predictive capacity when controlling for other groups of variables). Broad scale dbMEMs (i.e., dbMEMs representing spatial structures at the national scale; SI Fig.S4) explained a greater proportion of variation in site richness and diversity than groups of dbMEMs representing spatial relationships at a smaller scale. This reflects the impact of broad abiotic gradients (e.g., climate, temperature) on patterns of floristic diversity across the United States. For example, MEM2, which by itself can predict 4% of variation in species richness, roughly corresponded to patterns of high, constant mean temperature in the southeast of the United States, and the more variable climate of the Midwest and West regions (SI Fig. S4). Mean annual temperature impacts resource availability and the length of growing seasons enabling species with different temporal niches to coexist while precipitations affect local salinity in turn modulating species composition based on their tolerance to these conditions (Feher et al., 2017; Osland et al., 2017). Meanwhile, fine and very fine scale dbMEMs explained a small, but significant proportion of species richness and diversity, which may reflect more regional constraints to diversity. Spatially structured land cover context, for example, isolating or otherwise promoting connectivity among wetland sites could modulate diversity at a more regional scale.

Finally, the significant predictive capacity of dbMEMs underlines their potential to help upscale local in situ floristic surveys into biodiversity estimates. While greenness and texture can help account for conditions favoring diversity at the site scale (e.g., habitat heterogeneity, presence of resource promoting both productivity and diversity), dbMEMs might help account for other regional conditions that further modulate patterns of richness. Using dbMEMs might thus refine predictions where species richness is lower or higher than its expected magnitude based on greenness and texture as a result of regional factors and exogenous controls.

4.3 Limitations

This study leveraged products from different sensors and at a vast scale, which inevitably brings certain challenges and limitations. First, there is a mismatch in the timing of field surveys, NAIP data acquisition, and peak greenness as determined from Landsat time series. Field monitoring occurred between April and November of 2011 (US EPA, 2016). As such, the timing of field monitoring may not fully represent conditions at the maximum greenness state used for this analysis (Taddeo et al., 2019a) or when the high resolution images used to derived texture metrics were captured (although all NAIP images have been acquired between April and October; SI Fig. S5). Our analysis reveals a strong correlation between in-situ field observations conducted during the first and second visit in a subsample of 96 sites (SI Table S1), consistent with observations made by the EPA (US EPA 2016), suggesting that field surveys may offer a reasonable approximation of floristic conditions at peak greenness. Furthermore, we used high-resolution aerial images captured in both 2010 (30 states) and 2011 (18 states) with the month of image acquisition differing by state (SI Fig. S5) and may consequently not correspond to the timing of maximum greenness approximated from Landsat time series nor the exact timing of field surveys. As such, it is possible that the textural metrics we are using in this dataset do not fully capture the spectral heterogeneity that would be observable at a different time of the year, particularly in sites in which species have a contrasted phenology. To assess the degree of seasonal variation in spectral heterogeneity, we plotted site-wide coefficient of variation in GNDVI (i.e., coefficient of variation in GNDVI across the nine Landsat cells overlapping NWCA sites) for the different months corresponding to NAIP image acquisition (SI Fig. S6). While the coefficient of variation in GNDVI in estuarine wetlands is fairly constant throughout the growing season (SI Fig. S6A), inland wetlands are characterized by a greater spatial variability in GNDVI values in early spring and fall, possibly due to an asynchrony in plant phenology (Fig. S6B). NAIP images acquired in inland wetlands in April, September, and October might thus be underestimating spectral heterogeneity.

5 Conclusion

Wetland biodiversity is globally threatened but increasingly important considering its support of key ecosystem functions and services. It is critical to offer a consistent, repeated, and reliable portrait of biological resources at a national scale to support the cost-effectively allocation of conservation resources. While hyperspectral and very high-resolution remote sensing datasets offer the best likelihood of successfully identifying individual species, recent publications have found that indicators of site greenness can help predict plant richness, due to their sensitivity to diversity-productivity relationships. Our results suggest that incorporating texture metrics sensitive to habitat heterogeneity and diversity of growth forms can amplify this potential and enhance diversity and richness predictions, particularly in sites in which depending solely on maximum greenness is challenging due to the prevalence of mixed pixels or a high coverage of non-native species. In addition, our study shows that integrating dbMEMs representing spatial relationships among sites might help upscale local site surveys into regional or national estimates of biodiversity by offering a substitute to spatially structured variables known to locally or regionally impact plant diversity.

Overall, our results together with several previous studies (Hernández-Stefanoni et al., 2012; Madonsela et al., 2017; Wood et al., 2013) show the benefit of incorporating remote sensing into national conservation and monitoring strategies. Remote sensing and in situ floristic surveys can be part of a holistic, dynamic program in which in situ biodiversity assessments help train and interpret remote sensing-based assessments, while remote sensing can be used to identify where further local field investigation is needed to confirm biodiversity hotspots or areas of rapid degradation and bridge temporal and spatial gaps in between field assessments. For instance, changes in the spectral characteristics of a site could reflect a shift in plant composition or increased background exposure all of which could warrant further field investigation. Spectral indicators could also track wetland diversity resources at the national or continental scale to highlight biodiversity hotspots which should be targeted by conservation and planning efforts. Similarly, repeated site assessments using remote sensing products could be used as a low-cost, rapid monitoring of the biological conditions in each wetland of a particular site or region.

Finally, novel machine learning approaches could improve the predictive capacity of similar multivariate models combining spatial and spectral variables to estimate plant diversity across large datasets and study extents (SI Fig. S7). Machine learning models are particularly well suited for the analysis of complex ecological datasets as they can account for both linear and non-linear relationships and typically rely on fewer assumptions than traditional linear regression models (Olden et al., 2008).

6 Acknowledgments

This research is partially supported by the National Aeronautics and Space Administration Grant No. 80NSSC18K0755 issued to Dr. Iryna Dronova through the New (Early Career) Investigator Program (NNH17ZDA001N-NIP, proposal No.17-NIP17-0069). We are grateful for the suggestions made by two anonymous reviewers who greatly improved the manuscript.

7 References

Andrew, M.E., Ustin, S.L., 2008. The role of environmental context in mapping invasive plants with hyperspectral image data. Remote Sens. Environ. 112, 4301–4317. doi:https://doi.org/10.1016/j.rse.2008.07.016

Andrew, M.E., Wulder, M. a., Nelson, T. a., 2014. Potential contributions of remote sensing to ecosystem service assessments. Prog. Phys. Geogr. 38, 328–353. doi:10.1177/0309133314528942

Asner, G.P., 1998. Biophysical and biochemical sources of variability in canopy reflectance. Remote Sens. Environ. 64, 234–253. doi:10.1016/S0034-4257(98)00014-5

Biswas, S.R., Mallik, A.U., Braithwaite, N.T., Wagner, H.H., 2016. A conceptual framework for the spatial analysis of functional trait diversity. Oikos 125, 192–200. doi:10.1111/oik.02277

Bradley, B.A., 2014. Remote detection of invasive plants: A review of spectral, textural and phenological approaches. Biol. Invasions 16, 1411–1425. doi:10.1007/s10530-013-0578-9

Cardinale, B.J., Duffy, J.E., Gonzalez, A., Hooper, D.U., Perrings, C., Venail, P., Narwani, A., Mace, G.M., Tilman, D., Wardle, D. a, Kinzig, A.P., Daily, G.C., Loreau, M., Grace, J.B., Larigauderie, A., Srivastava, D.S., Naeem, S., 2012. Biodiversity loss and its impact on humanity. Nature 486, 59–67. doi:10.1038/nature11148

Castillo-Riffart, I., Galleguillos, M., Lopatin, J., Perez-Quezada, J.F., 2017. Predicting vascular plant diversity in anthropogenic peatlands: Comparison of modeling methods with free satellite data. Remote Sens. 9, 681. doi:10.3390/rs9070681

Chmura, G.L., Anisfeld, S.C., Cahoon, D.R., Lynch, J.C., 2003. Global carbon sequestration in tidal, saline wetland soils. Global Biogeochem. Cycles 17, 12. doi:1111 10.1029/2002gb001917

Costanza, R., Perez-Maqueo, O., Luisa Martinez, M., Sutton, P., Anderson, S.J., Mulder, K., 2008. The value of coastal wetlands for hurricane protection. Ambio 37, 241–248. doi:10.1579/0044-

7447(2008)37{[}241:TVOCWF]2.0.CO;2

Craft, C., Clough, J., Ehman, J., Joye, S., Park, R., Pennings, S., Guo, H., Machmuller, M., 2009. Forecasting the effects of accelerated sea-level rise on tidal marsh ecosystem services. Front. Ecol. Environ. 7, 73–78. doi:10.1890/070219

Davidson, N.C., 2014. How much wetland has the world lost? Long-term and recent trends in global wetland area. Mar. Freshw. Res. 65, 934–941. doi:10.1071/MF14173

Deutschewitz, K., Lausch, A., Kuhn, I., Klotz, S., 2003. Native and alien plant species richness in relation to spatial heterogeneity on a regional scale in Germany. Glob. Ecol. Biogeogr. 12, 299–311. doi:10.1046/j.1466-822X.2003.00025.x

Dray, S., Bauman, D., Blanchet, G., Borcard, D., Clappe, S., Guenard, G., Jombart, T., Larocque, G., Legendre, P., Madi, N., Wagner, H.H., 2018. Adespatial: Multivariate Multiscale Spatial Analysis. R package version 0.3-2.

Dray, S., Legendre, P., Peres-Neto, P.R., 2006. Spatial modelling: a comprehensive framework for principal coordinate analysis of neighbour matrices (PCNM). Ecol. Modell. 196, 483–493. doi:10.1016/j.ecolmodel.2006.02.015

Dudgeon, D., Arthington, A.H., Gessner, M.O., Kawabata, Z.I., Knowler, D.J., Lévêque, C., Naiman, R.J., Prieur-Richard, A.H., Soto, D., Stiassny, M.L.J., Sullivan, C.A., 2006. Freshwater biodiversity: Importance, threats, status and conservation challenges. Biol. Rev. Camb. Philos. Soc. 81, 163–182. doi:10.1017/S1464793105006950

Feher, L.C., Osland, M.J., Griffith, K.T., Grace, J.B., Howard, R.J., Stagg, C.L., Enwright, N.M., Krauss, K.W., Gabler, C.A., Day, R.H., Rogers, K., 2017. Linear and nonlinear effects of temperature and precipitation on ecosystem properties in tidal saline wetlands. Ecosphere 8, e01956. doi:10.1002/ecs2.1956

Feilhauer, H., He, K.S., Rocchini, D., 2012. Modeling Species Distribution Using Niche-Based Proxies Derived from Composite Bioclimatic Variables and MODIS NDVI. Remote Sens. 4, 2057–2075. doi:10.3390/rs4072057

Gibbs, J.P., 2011. Wetland Loss and Biodiversity Conservation. Conserv. Biol. 14, 314–317. doi:10.1007/s10531-011-0010-7

Gitelson, A.A., Merzlyak, M.N., 1998. Remote sensing of chlorophyll concentration in higher plant leaves. Adv. Sp. Res. 22, 689–692. doi:10.1016/S0273-1177(97)01133-2

Gorelick, N., Hancher, M., Dixon, M., Ilyushchenko, S., Thau, D., Moore, R., 2017. Google Earth Engine: Planetary-scale geospatial analysis for everyone. Remote Sens. Environ. 202, 18–27. doi:10.1016/j.rse.2017.06.031

Gould, W., 2000. Remote Sensing of Vegetation, Plant Species Richness, and Regional Biodiversity Hotspots. Ecol. Appl. 10, 1861–1870.

Guo, X., Wilmshurst, J., McCanny, S., Fargey, P., Richard, P., 2004. Measuring Spatial and Vertical Heterogeneity of Grasslands Using Remote Sensing Techniques. J. Environ. INFORMATICS 3, 24–32. doi:10.3808/jei.200400024

Hall-Beyer, M., 2017. Practical guidelines for choosing GLCM textures to use in landscape classification tasks over a range of moderate spatial scales. Int. J. Remote Sens. 38, 1312–1338. doi:10.1080/01431161.2016.1278314

Hall-Beyer, M., 2007. GLCM Texture: A Tutorial v. 1.0 through 2.7. doi:http://dx.doi.org/10.11575/PRISM/33280

Haralick, R.M., 1979. Statistical and structural approaches to texture. Proc. IEEE 67, 786–804. doi:10.1109/PROC.1979.11328

Hernández-Stefanoni, J.L., Gallardo-Cruz, J.A., Meave, J.A., Rocchini, D., Bello-Pineda, J., López-Martínez, J.O., 2012. Modeling (α- and β-diversity in a tropical forest from remotely sensed and spatial data. Int. J. Appl. Earth Obs. Geoinf. 19, 359–368. doi:10.1016/j.jag.2012.04.002

Hooper, D.U., Adair, E.C., Cardinale, B.J., Byrnes, J.E.K., Hungate, B.A., Matulich, K.L., Gonzalez, A., Duffy, J.E., Gamfeldt, L., Connor, M.I., 2012. A global synthesis reveals biodiversity loss as a major driver of ecosystem change. Nature 486, 105–108. doi:10.1038/nature11118

Hooper, D.U., Chapin, F.S.I., Ewel, J.J., 2005. Effects of biodiversity on ecosystem functioning: a consensus of current knowledge. Ecol. Monogr. 75, 3–35. doi:10.1890/04-0922

Huete, A.R., Jackson, R.D., Post, D.F., 1985. Spectral response of a plant canopy with different soil backgrounds. Remote Sens. Environ. 17, 37–53. doi:https://doi.org/10.1016/0034-4257(85)90111-7

Huete, A.R., Liu, H.Q., Batchily, K., VanLeeuwen, W., 1997. A comparison of vegetation indices global set of TM images for EOS-MODIS. Remote Sens. Environ. 59, 440–451. doi:10.1016/S0034-4257(96)00112-5

Karst, J., Gilbert, B., Lechowicz, M.J., 2005. Fern Community Assembly: The Roles of Chance and the

Environment at Local and Intermediate Scales. Ecology 86, 2473–2486. doi:10.1890/04-1420

Kingsford, R.T., Basset, A., Jackson, L., 2016. Wetlands: conservation's poor cousins. Aquat. Conserv. Mar. Freshw. Ecosyst. 26, 892–916. doi:10.1002/aqc.2709

Kreft, H., Jetz, W., 2007. Global patterns and determinants of vascular plant diversity. Proc. Natl. Acad. Sci. U. S. A. 104, 5925–5930. doi:10.1073/pnas.0608361104

Madonsela, S., Cho, M.A., Ramoelo, A., Mutanga, O., 2017. Remote sensing of species diversity using Landsat 8 spectral variables. ISPRS J. Photogramm. Remote Sens. 133, 116–127. doi:10.1016/j.isprsjprs.2017.10.008

Niering, W.A., 1988. Endangered, Threatened and Rare Wetland Plants and Animals of the Continental United States, in: The Ecology and Management of Wetlands: Volume 1: Ecology of Wetlands. Springer US, New York, NY, pp. 227–238. doi:10.1007/978-1-4684-8378-9_19

Oksanen, J., Blanchet, G., Friendly, M., Kindt, R., Legendre, P., McGlinn, D., Minchin, P.R., O'Hara, R.B., Simpson, G.L., Solymos, P., Steve, M.H.H., Szoecs, E., Wagner, H.H., 2019. vegan: Community Ecology Package.

OLDEN, J.D., LAWLER, J.J., POFF, N.L., 2008. Machine learning methods without tears: a primer for ecologists. Q. Rev. Biol. 83, 171–193.

Osland, M.J., Feher, L.C., Griffith, K.T., Cavanaugh, K.C., Enwright, N.M., Day, R.H., Stagg, C.L., Krauss, K.W., Howard, R.J., Grace, J.B., Rogers, K., 2017. Climatic controls on the global distribution, abundance, and species richness of mangrove forests. Ecol. Monogr. 87, 341–359. doi:10.1002/ecm.1248

Palmer, M.W., Earls, P.G., Hoagland, B.W., White, P.S., Wohlgemuth, T., 2002. Quantitative tools for perfecting species lists. Environmetrics 13, 121–137. doi:10.1002/env.516

Pereira, H.M., Daily, G.C., 2006. Modeling Biodiversity Dynamics in Countryside and Native Habitats. Ecology 87, 1877–1885. doi:10.1016/B978-0-12-384719-5.00334-8

Pereira, H.M., Ferrier, S., Walters, M., Geller, G.N., Jongman, R.H.G., Scholes, R.J., Bruford, M.W., Brummitt, N., Butchart, S.H.M., Cardoso, A.C., Coops, N.C., Dulloo, E., Faith, D.P., Freyhof, J., Gregory, R.D., Heip, C., Hoft, R., Hurtt, G., Jetz, W., Karp, D.S., McGeoch, M.A., Obura, D., Onoda, Y., Pettorelli, N., Reyers, B., Sayre, R., Scharlemann, J.P.W., Stuart, S.N., Turak, E., Walpole, M., Wegmann, M., 2013. Essential Biodiversity Variables. Science (80-.). 339, 277–278. doi:10.1126/science.1229931

Peres-Neto, P.R., Legendre, P., 2010. Estimating and controlling for spatial structure in the study of ecological communities. Glob. Ecol. Biogeogr. 19, 174–184. doi:10.1111/j.1466-8238.2009.00506.x

Rizzo, M.L., Székely, G., 2018. energy: E-Statistics: Multivariate Inference via the Energy of Data.

Schmidt, K.S., Skidmore, A.K., 2003. Spectral discrimination of vegetation types in a coastal wetland. Remote Sens. Environ. 85, 92–108. doi:10.1016/S0034-4257(02)00196-7

Shepard, C.C., Crain, C.M., Beck, M.W., 2011. The protective role of coastal marshes: A systematic review and meta-analysis. PLoS One 6. doi:10.1371/journal.pone.0027374

Székely, G.J., Rizzo, M.L., Bakirov, N.K., 2007. Measuring and testing dependence by correlation of distances. Ann. Stat. 35, 2769–2794. doi:10.1214/009053607000000505

Taddeo, S., Dronova, I., Depsky, N., 2019a. Remote Sensing of Environment Spectral vegetation indices of wetland greenness : Responses to vegetation structure , composition , and spatial distribution. Remote Sens. Environ. 234, 111467. doi:10.1016/j.rse.2019.111467

Taddeo, S., Dronova, I., Harris, K., 2019b. The potential of satellite greenness to predict plant diversity among wetland types, ecoregions, and disturbance levels. Ecol. Appl. 29, e01961. doi:10.1002/eap.1961

Tilman, D., Wedin, D., Knops, J., 1996. Productivity and sustainability influenced by biodiversity in grassland ecosystems. Nature 379, 718–720. doi:10.1038/379718a0

Todd, S.W., Hoffer, R.M., 1998. Responses of Spectral Indices to Variations in Vegetation Cover and Soil Background. Photogramm. Eng. Remote Sensing 64, 915–921.

Turner, W., Spector, S., Gardiner, N., Fladeland, M., Sterling, E., Steininger, M., 2003. Remote sensing for biodiversity science and conservation. TRENDS Ecol. Evol. 18, 306–314. doi:10.1016/S0169-5347(03)00070-3

US EPA, 2016. National Wetland Condition Assessment: 2011 Technical Report. Washington, DC.

Ustin, S.L., Gamon, J. a., 2010. Remote sensing of plant functional types. New Phytol. 186, 795–816. doi:10.1111/j.1469-8137.2010.03284.x

Wood, E.M., Pidgeon, A.M., Radeloff, V.C., Keuler, N.S., 2013. Image Texture Predicts Avian Density and Species Richness. PLoS One 8. doi:10.1371/journal.pone.0063211

Zedler, J.B., 2003. Wetlands at your service : reducing impacts of agriculture at the watershed scale. Front. Ecol. Environ. 1, 65–72.

Table 3. Adjusted R^2 and Akaike information criterion (AIC) for linear regressions between maximum annual greenness, texture metrics, combinations of greenness and texture, dbMEMs, a combination of spectral and spatial metrics ("all") species richness, and diversity, by wetland type and disturbance level. Stars indicate p-value, where: *: p <= 0.05; **: p <= 0.01; ***: p <= 0.001; ****: p <= 0.0001.

Dataset	**Diversity Index**	**Greenness**		**Texture**		**Texture + Greenness**		**Texture * Greenness**		**dbMEMs**		**All**	
		$AdjR^2$	AIC	$AdjR^2$	AIC	$AdjR^2$	AIC	$AdjR^2$	AIC	$AdjR^2$	AIC	$AdjR^2$	AIC
All sites	Diversity	0.33***	2284.63	0.35***	2267.50	0.45***	2091.42	0.47***	2065.36	0.14***	2594.78	0.50***	2155.72
	Total Richness	0.44***	2433.46	0.36***	2590.66	0.53***	2253.19	0.55***	2219.39	0.23***	2799.64	0.59***	2153.13
	Native Richness	0.43***	2443.64	0.36***	2574.99	0.52***	2261.61	0.54***	2237.46	0.23***	2798.02	0.58***	2140.87
Least disturbed sites (n=273)	Diversity	0.50***	534.90	0.42***	590.30	0.57***	507.45	0.58***	518.95	0.31***	667.44	0.60***	530.02
	Total Richness	0.57***	618.93	0.45***	699.99	0.65***	578.04	0.66***	587.55	0.45***	727.41	0.71***	570.70
	Native Richness	0.56***	608.21	0.45***	682.24	0.64***	569.26	0.65***	578.69	0.43***	718.95	0.70***	562.66
Intermediate disturbed sites (n=518)	Diversity	0.29***	1007.98	0.29***	1138.65	0.39***	943.53	0.42***	935.22	0.20***	1162.20	0.46***	972.55
	Total Richness	0.39***	1045.72	0.32***	1119.29	0.46***	998.24	0.48***	992.78	0.26***	1238.62	0.55***	991.63
	Native Richness	0.38***	1061.43	0.29***	1148.05	0.45***	1017.02	0.47***	1012.18	0.26***	1252.15	0.54***	1011.42
Most disturbed sites (n=324)	Diversity	0.20***	723.10	0.39***	649.20	0.43***	630.47	0.47***	619.39	0.37***	697.27	0.58***	577.59
	Total Richness	0.29***	743.00	0.40***	700.00	0.48***	654.78	0.53***	642.08	0.39***	746.81	0.60***	618.10
	Native Richness	0.31***	758.68	0.44***	704.20	0.53***	652.03	0.56***	646.62	0.43***	747.89	0.64***	613.98
Estuarine woody (n=70)	Diversity	0.12**	119.39	0.26**	120.52	0.31**	116.60	0.35**	118.26	0.38***	102.24	0.39**	112.29
	Total Richness	0.13**	134.88	0.32**	130.97	0.42**	119.97	0.50**	116.00	0.50***	103.12	0.52***	110.66
	Native Richness	0.12*	135.63	0.31**	132.03	0.41**	121.54	0.46**	121.45	0.47***	108.23	0.50***	114.83
Estuarine herbaceous (n=270)	Diversity	0.12***	459.88	0.14***	470.08	0.20***	450.15	0.20***	464.40	0.11***	477.20	0.29***	433.18
	Total Richness	0.23***	535.94	0.17***	572.93	0.32***	518.33	0.35***	520.92	0.14***	582.37	0.39***	504.00
	Native Richness	0.18***	538.42	0.16***	559.59	0.27***	521.51	0.33***	513.53	0.12***	570.21	0.34***	510.49
Inland herbaceous (n=350)	Diversity	0.05***	717.28	0.07**	724.33	0.10***	716.83	0.11***	728.78	0.11**	757.30	0.21***	730.48
	Total Richness	0.13***	686.43	0.11***	721.11	0.20***	687.46	0.22***	695.97	0.16***	747.42	0.30***	697.63
	Native Richness	0.17***	734.22	0.13***	767.35	0.21***	734.02	0.24***	735.7	0.22***	775.06	0.36***	790.97
Inland woody (n=425)	Diversity	0.07***	621.03	0.14***	602.38	0.18***	582.95	0.21***	585.13	0.14**	672.52	0.29***	603.79
	Total Richness	0.10***	660.04	0.12***	666.40	0.18***	634.26	0.20***	639.73	0.18***	703.37	0.31***	640.56
	Native Richness	0.15***	666.99	0.12***	692.67	0.22***	642.42	0.25***	643.87	0.22***	710.55	0.35***	643.74